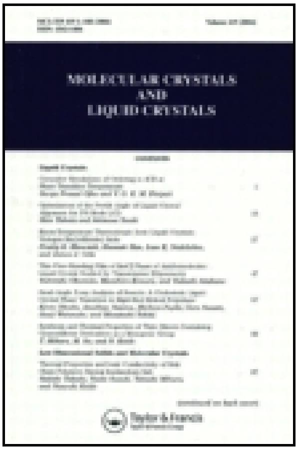

Molecular Crystals and Liquid Crystals Science and Technology. Section A. Molecular Crystals and Liquid Crystals

Publication details, including instructions for authors and subscription information:
http://www.tandfonline.com/loi/gmcl19

Switching Characteristics of Hybrid Aligned Ferroelectric Liquid Crystals under Horizontal Electric Field

Morichika Takata [a], Hiroyuki Okada [a] & Hiroyoshi Onnagawa [a]

[a] Faculty of Engineering, Toyama University, 3190 Gofuku, Toyama, 930-8555, Japan

Version of record first published: 24 Sep 2006

Mol. Cryst. and Liq. Cryst., 2001, Vol. 367, pp. 825-832
Reprints available directly from the publisher
Photocopying permitted by license only

Switching Characteristics of Hybrid Aligned Ferroelectric Liquid Crystals under Horizontal Electric Field

MORICHIKA TAKATA, HIROYUKI OKADA and HIROYOSHI. ONNAGAWA

Faculty of Engineering, Toyama University, 3190 Gofuku, Toyama 930-8555, Japan

Switching characteristics of ferroelectric liquid crystals under horizontal electric field have been investigated. In order to stabilize a single domain state, hybrid alignment was employed. In order to reduce a hysteresis in transmittance versus voltage characteristics, short-pitch ferroelectric liquid crystal materials were useful. Obtained contrast ratio was 10:1. Optical response showed mono-stable behavior and transmittance rise and fall times were 220 and 150 μs, respectively.

Keywords: Ferroelectric liquid crystals; hybrid alignment; single domain; mono-stable; horizontal electric field

Introduction

Ferroelectric liquid crystal (FLC) is interesting for its short response time. Early research works were mainly focused on the surface stabilized ferroelectric liquid crystals for multiplexing addressing scheme. [1] Recently, active matrix addressed ferroelectric liquid crystals have been investigated. [2,3] In the previous report, we have reported switching characteristics of ferroelectric liquid crystals under horizontal electric field. [4,5] In this experiment, we used conventional surface stabilized structure. Due to the structure, dual domains were formed and transmittance versus voltage characteristics showed hysteresis. In this time, we have investigated *a hybrid aligned* FLCs and have evaluated the switching characteristics under horizontal electric field.

Table 1. Data of alignment layers

Alignment layer	θ_p (deg)	γ_s^d (mN/m)	γ_s^p (mN/m)	γ_s (mN/m)
PAN	3.2	18.3	20.4	38.7
ZSA	3.5	27.0	10.7	37.7
PPO	10.0	33.2	0.3	33.5
2401	14.0	37.2	0.1	37.3

Table 2. Liquid crystal materials under study

Compounds	Type	Transition Temperature (℃)	Ps (nC/cm^2)	Tilt Angle θ (deg)	pitch p (μm)	response (μs)
CS-1024	FLC	Cryst(-12)S_C*(62)S_A(82)N*(90)Iso	-46.9	25	>20	73
CS-1031	FLC	Cryst(-12)S_C*(61.3)S_A(84.8)N*(96.2)Iso	28.1	19.3	3	26
TM-C103	FLC	S_C*(62.4)S_A(79.5)N*(91.3)Iso	20.1	25.9	>20	65
TM-C104	FLC	S_C*(63)S_A(76)N*(91.6)Iso	7.8	24.8	>20	134
CS-1017	FLC	Cryst(-20)S_C*(55.6)S_A(64.0)N*(68.7)Iso	-9.3	26	1	184
CS-2004	FLC (large θ)	Cryst(-9)S_C*(62)N*(71)Iso	-68.7	44	15	274
CS-4001	AFLC	S_{CA}*(66.8)$S_{C\gamma}$*(67.8)S_C*(70.1)S_A(86.0)Iso	79.7	24.9	/	79.5
TM-C108	SA	S_C*(20.9)S_A(75.2)Iso	/	17	/	/

In order to obtain a uniform and mono-stable alignment state, the hybrid alignment, in which the alignment layer materials of opposite glass substrates were different, was used. Pretilt angles and surface energies of the alignment layers from contact angle measurement of Wilhelmy method are listed in Table 1. Polyacrylonitrile (PAN) showed larger polar component of surface energy, PSI-G-4001 (ZSA: Chisso), PSI-A-2001 (PPO: Chisso) and PSI-A-2401 (2401: Chisso) were polyimides. Especially in PPO and 2401, high-pretilt angles and smaller polar component of surface energies were obtained. Properties of the liquid crystal materials used are also listed in Table 2. Where, CS-1024, TM-C103 and TM-C104 are mixture of rectus and sinister enantiomers with the same core structure.

Cross sectional and plane view of the liquid crystal cell are shown in Fig.1. Electrode material was tantalum covered with sputtered silicon dioxide. Electrode width *W* was 3 μm. The electrode spacing *S* was 7 μm for comparison of transmittance versus voltage (Tr-V) characteristics, and 2 μm for response measurement. Optical microscope with photomultiplier was used for Tr-V characteristics. Applied waveform was triangular and its frequency was 30 Hz. For optical response measurement, half duty cycle of rectangular waveform with bipolar polarity was applied. Based on Tsuchiya's analysis [6], surface and free energy calculation were carried out.

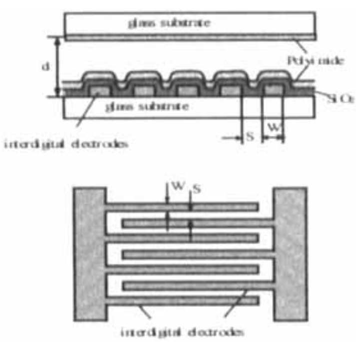

Figure 1. Cell configuration

Energy calculation for hybrid alignment

Referring Tsuchiya's analysis [6], a surface energy of dispersive and a polar interaction in hybrid alignment cell is described as

$$F_s = \sum \{\gamma_n(\vec{n}\bullet\vec{g})^2 + \gamma_p(\vec{p}\bullet\vec{g})\}$$
$$= (\gamma_{nu}\sin^2\phi_u + \gamma_{nl}\sin^2\phi_l)\sin^2\theta + (\gamma_{pu}\cos\ \phi_u + \gamma_{pl}\cos\phi_l)\frac{P_s}{|P_s|}, \qquad (1)$$

where, Σ is the sum of energy for upper and lower substrates, *n*, *p* and *g* are the unit vectors of n director, spontaneous polarization and substrate normal, respectively. And ϕ is the azimuthal angle of c-director, θ is the tilt angle and γ_n and γ_p are the surface energy of dispersive and polar component, respectively, where, *u* and *l* means upper and lower, respectively.

For uniform state of hybrid alignment, the surface energy between ϕ_s $(=\phi_u=\phi_l)=\pi$ and $\phi_s(=\phi_u=\phi_l)=0$ is different and the second term of Eq.(1) is as

$$F_{s,0}{}^U = (\gamma_{pu}-\gamma_{pl})\frac{P_s}{|P_s|}, \quad (\phi_s=0) \quad F_{s,\pi}{}^U = (-\gamma_{pu}+\gamma_{pl})\frac{P_s}{|P_s|}. \quad (\phi_s=\pi) \qquad (2)$$

We assumed $\gamma_{pu} > \gamma_{pl}$ and $P_S > 0$

$$F_{s,0}{}^U = (\gamma_{pu}-\gamma_{pl}) > 0, \qquad F_{s,\pi}{}^U = (-\gamma_{pu}+\gamma_{pl}) < 0.$$

Therefore, the $\phi=\pi$ was stabilized. On the other hand, $P_S<0$, then

$$F_{s,0}{}^U = -(\gamma_{pu}-\gamma_{pl}) < 0, \qquad F_{s,\pi}{}^U = -(-\gamma_{pu}+\gamma_{pl}) > 0.$$

Therefore, the $\phi=0$ was stabilized. As a whole, mono-domain state will be stabilized for hybrid alignment with different polar component.

Next, we consider the free energy calculation of hybrid aligned cell refer to Tsuchiya's analysis [6]. Assuming a c-director is constant, energy of helix state is as

$$F_t{}^H = \frac{\gamma_{nu}+\gamma_{nl}}{2}\sin^2\theta. \qquad (3)$$

Under uniform state, $\phi_u=\phi_l=\phi_{s0}$. As surface energy is minimum at $\phi=0$ or $\phi=\pi$, the energy is described as

$$F_t^u = \frac{1}{2}q_0{}^2 d(K_2+K_3-\widetilde{K})\sin^2\theta + (-\gamma_{pu}+\gamma_{pl}), \qquad (4)$$

where, $\gamma_{pu} > \gamma_{pl}$, $\phi_s=0$ $(P_S<0)$ and $\phi_s=\pi$ $(P_S>0)$.

For twist state, the energy is as

$$
\begin{aligned}
F_t^T = \int_{-\frac{d}{2}}^{\frac{d}{2}} [& \frac{1}{2}\phi_y{}^2 \sin^2\theta\left(K_1\cos^2\phi + \widetilde{K}\sin^2\phi\right) \\
& - \phi_y q_0 \left(K_3 - K_2\right)\sin^3\theta\cos\theta\sin\phi \\
& + \frac{1}{2} q_0{}^2 \sin^2\theta\left(K_2 + K_3 - \widetilde{K}\right)dy \\
& + \left(\gamma_{nu} + \gamma_{nl}\right)\sin^2\phi_s\sin^2\theta - \left(\gamma_{pu} + \gamma_{pl}\right)\cos\phi_s
\end{aligned}
\qquad (5)
$$

where, $\gamma_{pu} > \gamma_{pl}$,

$$\phi_l = \pi - \phi_u. \qquad \left(\frac{\pi}{2} < \phi_s < \frac{3\pi}{2}(P_s > 0), \quad -\frac{\pi}{2} < \phi_s < \frac{\pi}{2}(P_s < 0)\right)$$

Figures 2(a)-(c) shows calculated thickness dependence of tilt angle. Figure 2(a) shows the case of ordinary alignment using PAN. Figure 2(b) shows the case of ordinary alignment using 2401. And Fig.2(c) shows the case of hybrid alignment using the combination of PAN and 2401. Elastic constants were K_{11}=27.3pN, K_{22}=21.4pN and K_{33}=29.4pN. These values were measured with CS-1024 under nematic temperature range using Gruler's procedure. [7] Spontaneous polarization, tilt angle and helical pitch were listed in Table 2. The ϕ_0 was $-\pi/2$ and q_0 was negative. In Fig.2 (a), critical thickness was smaller than that of the case in Fig.2 (b). Therefore, the cell with PAN alignment layer show twisting tendency. This tendency was qualitatively in agreement with experimental results. The characteristics of 2401 case were almost similar to that of PAN/2401 hybrid alignment case. It is considered that the alignment condition of hybrid alignment case

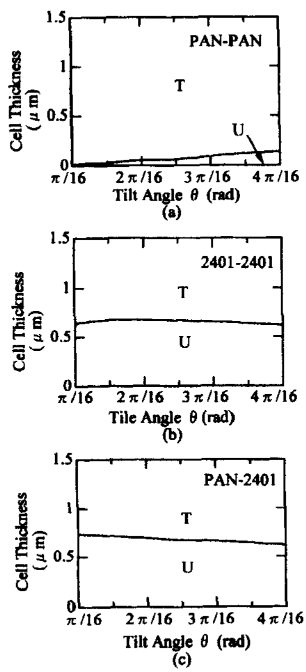

Figure 2. Calculated thickness dependence of the tilt angle.

largely affected to the stable alignment layer. Moreover, the critical thickness of the PAN/2401 hybrid alignment case was slightly larger than that of the case in 2401 for lower tilt angle. In the practical cells, the critical cell thickness was about 3 μm. This result was not well explained in this calculation. This discrepancy was due to a few percentage of the energy difference between twist and uniform states around one micron and the assumption that actual surface energy was slightly different from liquid crystal itself. Anyway, the twisting tendency was explained according to the polar component of the surface energy.

Experimental results

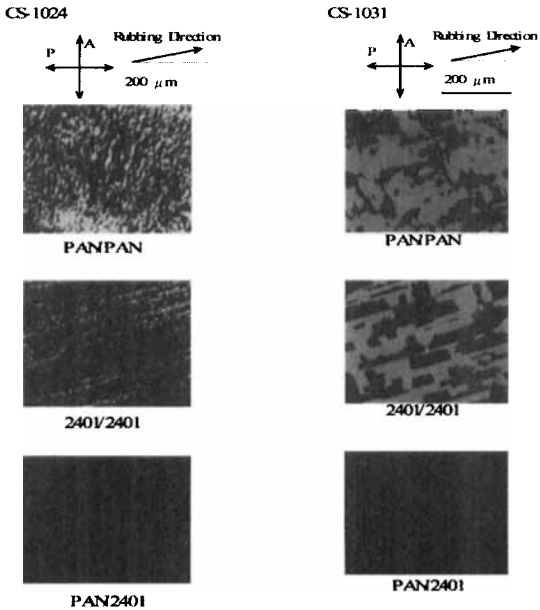

Figure 3. Examples of the alignment conditions

Figure 3 shows the examples of the alignment conditions. Upper, middle and lower photographs were PAN/PAN (ordinary), 2401/2401 (ordinary) and PAN/2401 (hybrid), respectively. Good mono-domain alignment was obtained in the hybrid alignment PAN/2401.

Table 3. Obtained alignment and extinction states

Upper Substrate	Lower Substrate	CS-1024			TM-C103			TM-C104			CS-1031		
		U1	U2	State	U1	U2	State	U1	U2	State	U1	U2	State
PAN	PAN	+13	-5	D	+13	-5	D	+11	-1	D	+14	-1	D
	ZSA	+14		S	+14		S	+11		S	+13		S
	PPO	+16		S	+15		S	+13		S	+14		S
	2401	+15		S	+15		S	+12		S	+13		S
ZSA	ZSA	+15	-5	D	+14	-8	D	+12	-2	D	+12	-4	D
	PPO	+16		S	+15		S	+12		S	+14		S
	2401	+14		S	+14		S	+12		S	+13		S
PPO	PPO	+16	-5	D	+13	-5	D	+13	-3	D	+16	-4	D
	2401	+14		S	+7		S	+15		S	+16		S
2401	2401	+14	-5	D	+13	-4	D	+15	-1	D	+15	-3	D

Table 3 shows obtained alignment and extinction states in the cell with parallel rubbing direction. The U1 and U2 mean uniform1 and uniform2 states, respectively. The value was the angle between rubbing direction and extinction condition. The symbols D and S means dual and single domains, respectively. As expected in the calculation, the single domain state was surprisingly realized by employing the hybrid alignment. The C-director model is shown in Fig.4.

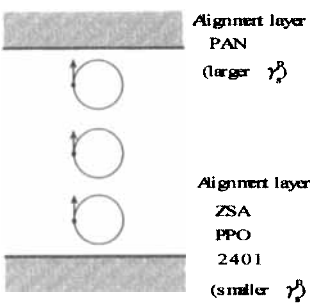

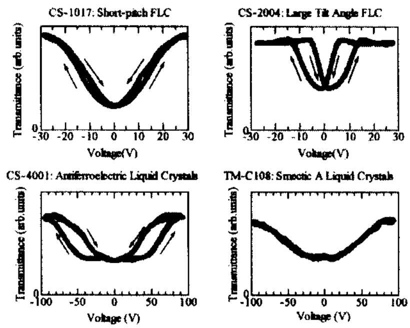

Figure 4. C-director model Figure 5. Tr-V curve for various LC materials

Comprehensive study about contrast ratios, hysteresis, symmetry of the Tr-V curve was carried out by changing the liquid crystal material, *i.e.*, short-pitch ferroelectric, large tilt angle ferroelectric, antiferroelectric and smectic *A* liquid crystal materials, as shown in Fig.5. Alignment layer was 2401 (electrode side)/ PAN. In the case of large tilt angle FLC and antiferroelectric LC, the Tr-V curves show hysteresis. In the case of smectic *A* LC, transmittance change was small. As a result of the investigations, the short-pitch FLC was the best.

In order to reduce the response time and the driving voltage, shorter electrode spacing was tested as follows.

The Tr-V Characteristics is shown in Fig.6. The transmittance was saturated above ± 15 V and symmetric Tr-V characteristics with varied voltage were obtained. Contrast ratio was 10:1. For lower frequencies, the hysteresis regarded as ions effect was observed. The switching phenomenon was non-uniform and the main part of switching was occurred near the electrodes edge. Therefore, this lower bright transmittance is the main reason for lower contrast ratio.

The response time was measured with rectangular waveform, as shown in Fig.7. The transmittance rise and fall times were 220 and 150 μs, respectively, under rectangular waveform at 20V. This value was almost same order as compared to conventional SSFLC cell.

Mono-stable characteristics were tested, as show in Fig.8. Upper trace was the waveform voltage and lower trace was the transmittance. The voltage increased between 0 to 20V. The transmittance gradually increased with increase in the voltage and the mono stable characteristics could be obtained.

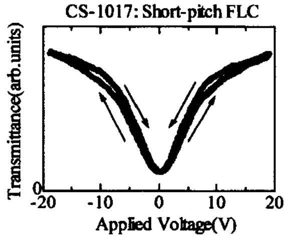

Figure 6. Tr-V characteristics

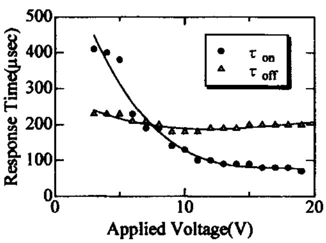

Figure 7. Response characteristics

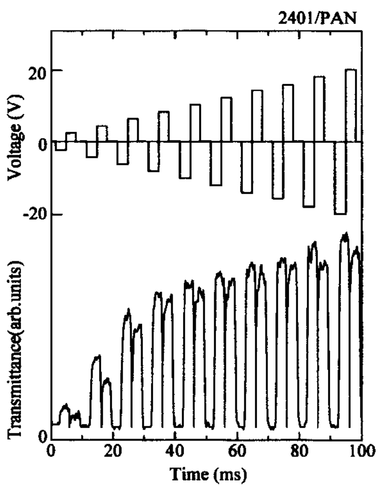

Figure 8. Optical response of mono-stable operation

Conclusion

We had investigated the switching characteristics of hybrid aligned ferroelectric liquid crystals under horizontal electric field. The hybrid alignment was essentially effective for uniform and mono-domain alignment. In addition, mono-stable operation was also confirmed for conventional SSFLC cell configuration. [8]

At present, contrast ratio was as low as 10:1. By solving the non-uniform switching problem, the FLC display performance under horizontal electric field will be improved.

Acknowledgment

The authors would like to thank Chisso Petrochemical Corp. for supplying liquid crystal and alignment materials.

References

[1] N.A. Clark and S.T. Lagerwall: Appl. Phys. Lett., 36, 899 (1980).
[2] M.D. Wand, and W.N. Thurmers, R.T. Vohra and K.M. More: Proc. 4 th Intl. Display Workshops (IDW'97) 89 (1997).
[3] K. Nito, T. Fujioka, N. Kataoka, A. Yasuda: Proc. AM-LCD, 48 (1994).
[4] M. Jian, H. Okada and H. Onnagawa: Technical Report of the Institute of Electronics, Information and Communication Engineering, EID95-148 (1996).
[5] M. Jian, M. Takata, S. Naka, H. Okada and H. Onnagawa: (will be published elsewhere).
[6] T. Tsuchiya, H. Takezoe and A. Fukuda: Jpn. J. Appl. Phys., 25, L27 (1986).
[7] H. Gruler, T.J. Scheffer and G. Meier: Z. Naturforsch, 27a, 966 (1972).
[8] K. Koshihara, H. Okada and H. Onnagawa: The 23 rd Spring Meeting of the Japan Society of Applied Physics, 2D05 (1997).